High-Temperature Superconductivity in $La_3Ni_2O_7$

Kun Jiang(蒋坤)[1,2], Ziqiang Wang(汪自强)[3], and Fu-Chun Zhang(张富春)[4,5]

[1]*Beijing National Laboratory for Condensed Matter Physics, and Institute of Physics, Chinese Academy of Sciences, Beijing 100190, China*
[2]*School of Physical Sciences, University of Chinese Academy of Sciences, Beijing 100190, China*
[3]*Department of Physics, Boston College, Chestnut Hill, MA 02467, USA*
[4]*Kavli Institute of Theoretical Sciences, University of Chinese Academy of Sciences, Beijing 100190, China*
[5]*Collaborative Innovation Center of Advanced Microstructures, Nanjing University, Nanjing 210093, China*

(Received 11 December 2023; accepted manuscript online 5 January 2024)

Motivated by the recent discovery of high-temperature superconductivity in bilayer $La_3Ni_2O_7$ under pressure, we study its electronic properties and superconductivity due to strong electron correlation. Using the inversion symmetry, we decouple the low-energy electronic structure into block-diagonal symmetric and antisymmetric sectors. It is found that the antisymmetric sector can be reduced to a one-band system near half filling, while the symmetric bands occupied by about two electrons are heavily overdoped individually. Using the strong coupling mean field theory, we obtain strong superconducting pairing with B_{1g} symmetry in the antisymmetric sector. We propose that due to the spin-orbital exchange coupling between the two sectors, B_{1g} pairing is induced in the symmetric bands, which in turn boosts the pairing gap in the antisymmetric band and enhances the high-temperature superconductivity with a congruent d-wave symmetry in pressurized $La_3Ni_2O_7$.

DOI: 10.1088/0256-307X/41/1/017402

The discovery of high-temperature (high-T_c) superconductivity in the cuprates,[1] whose transition temperatures greatly exceed conventional superconductors, encourages exploring none-copper-based high-T_c superconductors both experimentally and theoretically.[2–8] Among this exploration, it was theoretically proposed that the nickelates could be a counterpart of the cuprates.[9–11] Owing to sustained efforts on the synthesis,[12–16] superconductivity was finally found in the "infinite-layer" nickelates (Sr,Nd)NiO_2 thin films,[17–19] opening the nickel age of superconductivity.[20]

Recently, a new type of bulk nickelate $La_3Ni_2O_7$ (LNO) single crystal was successfully synthesized.[21] A high-temperature superconducting transition $T_c \sim 80\,\mathrm{K}$ under high pressure was reported.[21–24] After its discovery, tremendous theoretical effort has been applied to this new material.[25–42] Similar to the bilayer cuprates, the essential part of LNO superconductor is the bilayer NiO_2 block,[21] as illustrated in Fig. 1(a). We label them as the top and bottom layers. Around each Ni site, six oxygen atoms form a standard octahedron. The two nearest neighbor octahedrons between the two layers are corner shared by one apical oxygen. The LNO at ambient pressure is in its *Amam* phase with the two octahedrons tilted. The phase evolves into the high-symmetry structure *Fmmm* phase under high pressure. The two octahedrons line up and superconductivity emerges around 14 GPa. The octahedra crystal fields split the Ni $3d$ orbitals into t_{2g} and e_g complexes, as shown in Fig. 1(b).

Counting the chemical valence in LNO, Ni is in the $(2Ni)^{5+}$ state ($Ni^{2.5+}$ per site). Notice that Ni is normally in its Ni^{2+} or Ni^{1+} state, such that further hole doping always adds holes into the oxygen.[43–46] Therefore, the low-energy states of LNO are formed by the mixing Ni e_g and O p states, similar to the Zhang–Rice singlet in hole doped cuprates.[47] To simplify the discussion, we will continue to use Ni $3d$ states for convenience. As shown in Fig. 1(b), the $(2Ni)^{5+}$ has fully occupied t_{2g} orbitals and the e_g orbitals host three electrons. In the following discussion, we label the $d_{x^2-y^2}$ and d_{z^2} orbitals as d^x and d^z, and the top and bottom layers as t and b.

Focusing on the partially occupied e_g orbitals and utilizing the results of density functional theory (DFT) calculations, the tight-binding (TB) model for LNO can be derived[25,29] in the basis $(d^x_{tk}, d^z_{tk}, d^x_{bk}, d^z_{bk})$ as

$$H(k) = \begin{pmatrix} H_t(k) & H_\perp(k) \\ H_\perp(k) & H_b(k) \end{pmatrix},$$
$$H_b(k) = H_t(k) = \begin{pmatrix} T^x_k & V_k \\ V_k & T^z_k \end{pmatrix},$$
$$H_\perp(k) = \begin{pmatrix} t^x_\perp & V'_k \\ V'_k & t^z_\perp \end{pmatrix}. \quad (1)$$

Here, $T^{x/z}_k = t^{x/z}_1\gamma_k + t^{x/z}_2\alpha_k + \epsilon^{x/z}$, $V_k = t^{xz}_3\beta_k$, $V'_k = t^{xz}_4\beta_k$ with $\gamma_k = 2(\cos k_x + \cos k_y)$, $\alpha_k = 4\cos k_x \cos k_y$, $\beta_k = 2(\cos k_x - \cos k_y)$, and interlayer coupling $t^x_\perp = 0.005\,\mathrm{eV}$, $t^z_\perp = -0.635\,\mathrm{eV}$. The corresponding hopping parameters can be found in Ref. [25] and in the Supplemental

© 2024 Chinese Physical Society and IOP Publishing Ltd

Material (SM). DFT calculations show that the interlayer coupling is significant in LNO, which is captured by the off-diagonal block $H_\perp(k)$ of the TB Hamiltonian in Eq. (1). The LNO under pressure has an inversion symmetry about the shared apical oxygen. This means that $H(k)$ is block-diagonalized in the eigen basis of inversion that exchanges the top and bottom layers,

$$\psi_{\rm S}^{\eta} = (d_{\rm t}^{\eta} + d_{\rm b}^{\eta})/\sqrt{2}, \tag{2}$$

$$\psi_{\rm A}^{\eta} = (d_{\rm t}^{\eta} - d_{\rm b}^{\eta})/\sqrt{2}, \tag{3}$$

where $\eta = x, z$. It is easy to verify that $(\psi_{\rm S}, \psi_{\rm A})$ block diagonalizes $H(k)$ into

$$H_{\rm TB}(k) = \begin{pmatrix} H_{\rm S}(k) & 0 \\ 0 & H_{\rm A}(k) \end{pmatrix}. \tag{4}$$

The $H_{\rm S}(k)$ and $H_{\rm A}(k)$ take the same form as $H_{\rm t}(k)$ and $H_{\rm b}(k)$ in Eq. (1) but with different hopping parameters, as listed in the SM.

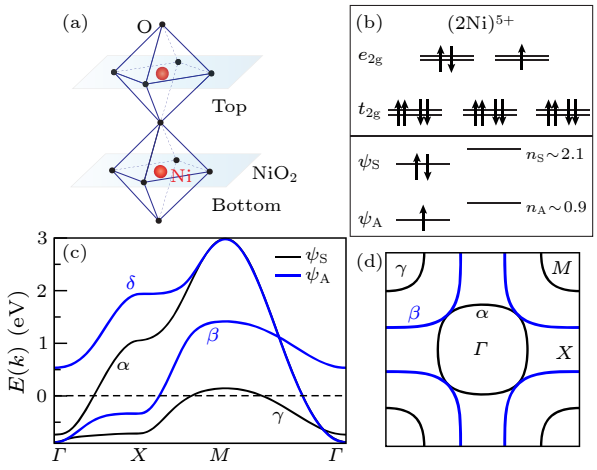

Fig. 1. (a) The essential part of the LNO structure. The bilayer NiO_2 plane, labeled as the top and bottom layers, is formed by two corner-shared NiO_6 octahedrons. (b) Upper: the occupation configuration in the $(2Ni)^{5+}$ state ($Ni^{2.5+}$). Lower: the occupation configuration of the symmetric $\psi_{\rm S}$ and antisymmetric $\psi_{\rm A}$ orbitals. (c) The low-energy band structure decoupled into two $\psi_{\rm S}$ bands (black) and two $\psi_{\rm A}$ bands (blue). (d) The corresponding Fermi surfaces labeled by α, β, and γ.

The TB electronic structure is plotted in Fig. 1(c), which is separated into two $\psi_{\rm S}$ bands (black lines) and two $\psi_{\rm A}$ bands (blue lines). There are three bands crossing the Fermi level, which are labeled by α, β, and γ with an unoccupied δ band. The Fermi surfaces (FSs) consist of one electron pocket (α) around the Γ point and two hole pockets (β, γ) around the M points in the Brillouin zone as shown in Fig. 1(d). Using these symmetric and antisymmetric orbitals, we find that the electron occupation number is quite interesting: $\psi_{\rm S}$ is occupied by closing to two electrons and $\psi_{\rm A}$ by closing to one electron, as summarized in Fig. 1(b). More precisely, the occupation in the anti-symmetric β band is around 0.91, while the symmetric γ band and α band are occupied by 1.725 and 0.365 electrons, respectively.

We start with the antisymmetric $\psi_{\rm A}$ bands shown in Fig. 2(a). Since the upper band is empty, we can project out the upper δ band and focus on the β band, which is close to half filling. The orbital content of the β band is dominated by the $d_{x^2-y^2}$ character in the DFT and the TB model. Hence, this is the band of the Zhang–Rice singlets.[47] The dispersion of the β band can be described by $t\gamma_k + t'\alpha_k + t''\gamma_{2k}$ with the effective nearest neighbor (t), next nearest neighbor (t'), and third neighbor hopping (t''), which is plotted (red line) in Fig. 2(a). The hopping parameters (t, t', t'') are given in the SM. The corresponding β-FS is shown in Fig. 2(b). Since the β band is about 10% hole doped away from half filling, the effects of local correlations are strong and captured by the one band t–J model,[2]

$$H_\beta = \sum_{ij} t_{ij} \hat{P} \psi^\dagger_{\beta,i\sigma} \psi_{\beta,j\sigma} \hat{P} + \sum_{\langle ij \rangle} J\Big(\boldsymbol{S}_i \cdot \boldsymbol{S}_j - \frac{1}{4} n_i n_j\Big). \tag{5}$$

Here $\hat{P}$ is the projection operator that removes double occupancy, J is the superexchange interaction and the Einstein summation notation over repeated indices is used.

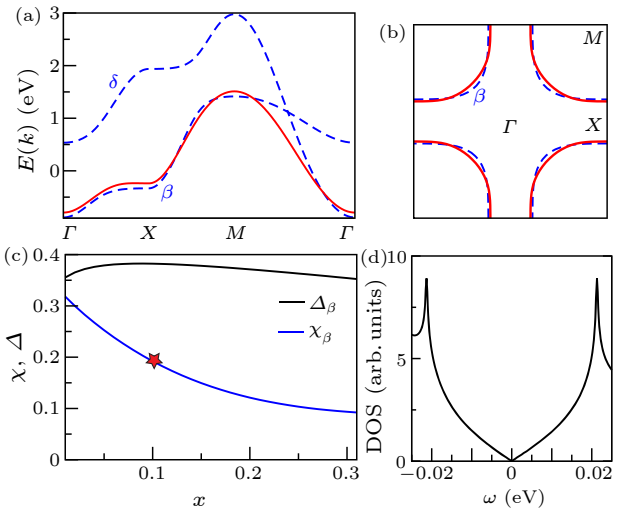

Fig. 2. The band structure (a) and FS (b) for the antisymmetric $\psi_{\rm A}$ bands plotted with blue dashed lines. The red solid lines correspond to those of the partially filled lower β band fitted with a single-band t–t'–t'' model, where $t = 0.288\,\text{eV}$, $t' = -0.0746\,\text{eV}$, $t'' = 0.04\,\text{eV}$. (c) The calculated mean-field order parameters χ_β and Δ_β versus hole doping x for exchange coupling $J = 0.12\,\text{eV}$. The red star marks $x = 0.1$ for the β band, where the tunneling DOS is calculated and plotted in (d).

The projection operator can be handled by writing $\psi_{\beta,i\sigma} = b_i^\dagger f_{i\sigma}$, where b_i is a slave-boson keeping track of empty sites and $f_{i\sigma}$ is a spin-1/2 fermion keeping track of singly occupied sites.[48] A physical constraint $b_i^\dagger b_i + f_{i\sigma}^\dagger f_{i\sigma} = 1$ is enforced here. Following the standard slave-boson mean-field theory,[2,48] H_β can be ap-

proximated as

$$H_\beta^{\rm MF} = \sum_{ij} \sqrt{x_i x_j} t_{ij} f_{i\sigma}^\dagger f_{j\sigma} + \frac{J}{4} \sum_{\langle ij \rangle} (|\chi_{ij}|^2 + |\Delta_{ij}|^2) - \frac{J}{4} \sum_{\langle ij \rangle} (\chi_{ij}^* f_{i\sigma}^\dagger f_{j\sigma} + \Delta_{ij}^* f_{i\sigma} f_{j\sigma'} \epsilon_{\sigma\sigma'} + \text{h.c.}), \quad (6)$$

where $\epsilon_{\sigma\sigma'}$ is the antisymmetric tensor, $\chi_{ij} = \langle f_{i\sigma}^\dagger f_{j\sigma} \rangle$ and $\Delta_{ij} = \epsilon_{\sigma\sigma'} \langle f_{i\sigma} f_{j\sigma'} \rangle$ are the mean-field nearest neighbor bond and spin-singlet pairing order parameters. The bosons b_i are condensed to expectation values $\sqrt{x_i}$, where x_i is the local doping concentration at site i. Choosing the homogeneous solution with $\chi_{ij} = \chi$ and $x_i = x$, we find that the B_{1g} pairing ansatz, with $\Delta_x = \Delta$ and $\Delta_y = -\Delta$ for bonds along x and y directions, is the ground state as in the cuprates.[2,49] The mean-field order parameters are self-consistently calculated and plotted in Fig. 2(c), as a function of the hole doping level x. For the β band filling around $x = 0.1$ [indicated by the red star in Fig. 2(c)], we obtain $\chi = 0.38$ and $\Delta = 0.19$. The calculated tunneling density of states (DOS) is shown in Fig. 2(d) at $x = 0.1$, exhibiting a large pairing gap of 21.3 meV. Thus, independent of the precise value of x, the closing to half-filled β band plays the leading role in the high temperature superconductivity in LNO.

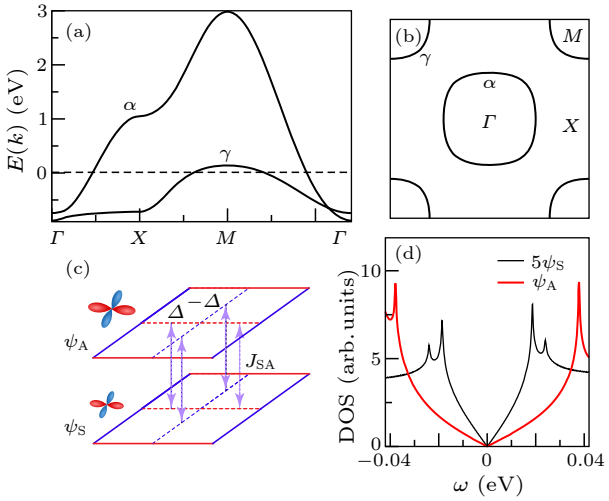

Fig. 3. (a) The band structure for the symmetric ψ_S bands. (b) The corresponding FSs for ψ_S bands. (c) The B_{1g} superconductivity for the symmetric ψ_S bands are induced by the antisymmetric ψ_A through the spin-orbital coupling interaction J_{SA}, forming a congruent d-wave pairing state. The pairing order parameters are positive on the red bonds and negative on the blue bonds. (d) The tunneling density of states for the coupling model with $J_{SA} = 0.05$ eV. The DOSs for ψ_S are magnified by a factor of 5 for visualization.

Next, we consider the inversion symmetric ψ_S bands and demonstrate that the high-T_c superconductivity is further enhanced in a congruent B_{1g} pairing state, such that the bilayer LNO can have a higher superconducting transition temperature T_c than a single-layer cuprate such as $La_{2-x}Sr_xCuO_4$ as observed experimentally.[21–23] The dispersion of the two ψ_S bands, with a filling fraction of $n_S \sim 2.1$, and the corresponding FSs are plotted in Figs. 3(a) and 3(b). As discussed above, there exist one hole-like γ FS corresponding to electron filling $n_\gamma = 1.725$ centered around the M point and one electron-like α FS with $n_\alpha = 0.365$ around the Γ point. This situation is similar to the iron-based superconductors and highly doped monolayer CuO_2 with the liberated d_{z^2} orbital.[50,51] If we only consider these two ψ_S bands, one could expect that an $S_\pm$ pairing shows up for the ψ_S bands. In order to explore this, a similar two-orbital slave-boson mean field theory by introducing slave bosons to ψ_S^x and ψ_S^z respectively has been applied to the ψ_S bands. From this mean-field study, we confirm that the leading pairing channel is A_{1g} with anti-phase $S_\pm$ order parameters at α and γ FSs. However, the pairing order parameters obtained here are 10 times smaller than the B_{1g} pairing order parameter in the β band. On the other hand, since the ψ_S bands are highly overdoped with respect to half filling in each band, the symmetric sector is far away from a doped Mott insulator and the effects of local correlation such as the band narrowing are relatively weak. As a result, the DOS of the whole system is dominated by the strongly renormalized antisymmetric β band. Hence, it is important to consider the coupling between the symmetric and antisymmetric sectors for the superconducting state of LNO.

Microscopically, although the inversion symmetry decouples the ψ_S and ψ_A bands for single-particle excitations, the Coulomb interactions couple the two sectors, as discussed in more detail in the SM. For our consideration, the most important symmetry allowed coupling is the spin-orbital exchange interaction,[50,51]

$$H_{\rm SAS} = J_{\rm SA} (\hat{\Delta}_{{\rm S}x}^\dagger \hat{\Delta}_{{\rm A}\beta} + \hat{\Delta}_{{\rm S}z}^\dagger \hat{\Delta}_{{\rm A}\beta} + \text{h.c.}), \quad (7)$$

which serves as an effective Josephson coupling between the pairing order parameters in the symmetric and antisymmetric sectors. Choosing a moderate $J_{SA} = 0.05$ eV and ignoring the weak band renormalization of the overdoped symmetric sector, we calculate the pairing order parameters self-consistently by solving for the ground state of $H_\beta^{\rm MF} + H_S^{\rm MF} + H_{\rm SAS}$ (see SM for more details). Intriguingly, the B_{1g} superconducting state in the β band, through the coupling J_{SA}, drives a congruent B_{1g} pairing state in the symmetric α and γ bands, as illustrated in Fig. 3(c). Specifically, all order parameters have a d-wave symmetry with amplitudes $(\Delta_{A,\beta}; \Delta_{S,x}, \Delta_{S,z}) = (0.24; 0.02, 0.04)$. The calculated tunneling DOS plotted in Fig. 3(d) shows that the contribution from the β band dominates and the spectral weight from the ψ_S bands is magnified by a factor of 5 for visualization. As clearly seen in Fig. 3(d), there are two energy gaps from the ψ_S bands at 24.0 meV and 18.7 meV. Remarkably, the DOS reveals a large gap around 37.9 meV from the β band, which is significantly larger than that produced by the uncoupled β band t–J model shown in Fig. 2(d). We thus conclude that exchange coupling the strongly correlated β band to the weakly corre-

lated α and γ bands with a large carrier density produces a congruent d-wave pairing state with boosted pairing energy gap and enhanced high-T_c superconductivity, which can be a novelty of LNO under pressure.

In summary, we have taken the viewpoint of strong interlayer hybridization and classified single electron state as symmetric ($k_z = 0$) or antisymmetric ($k_z = \pi$) linear combination of the state on top and bottom layers. We then introduce a large "on-site" Coulomb repulsion in the single electron Hamiltonian for the symmetric and antisymmetric states, here a "site" means a molecule site consisting of two crystal sites with one in the top and one in the bottom layer. The Hamiltonian for the antisymmetric states describes a near half-filled hole doped t–t'–t''–J model on a square lattice for predominantly Ni $3d_{x^2-y^2}$ orbitals, which gives d-wave superconductivity, similar to superconductivity found in cuprates[3] and proposed in $LaNiO_3/LaMO_3$ superlattices.[11] The Hamiltonian for symmetric states describes a nearly full-filled predominantly $3d_{z^2}$ orbital band and a lightly filled predominantly $3d_{x^2-y^2}$ orbital band, which do not appear to play dominant roles in superconductivity on their own. We argued by explicit calculations that the spin-orbital exchange coupling between the symmetric and antisymmetric sectors can drive a congruent d-wave pairing state with significantly boosted superconducting energy gap and thus enhanced transition temperature T_c, beyond those of the typical single-layer cuprates. This scenario agrees with the electron band calculations for the normal state.[21,25,29] Note that we have examined the Fermi surfaces based on the finite-U Gutzwiller approximation and found that they remain approximately the same (see the SM for more details). A recent angle-resolved photoemission spectroscopy measurement at ambient pressure shows that the measured band dispersion of $La_3Ni_2O_7$ is consistent with the band calculations.[52] Hence, the filling to each band, especially the β band, is still around the band calculation result. Our starting point from the symmetric and antisymmetric bands is justified. On the other hand, the inversion symmetry between the top and bottom NiO_2 layers with respect to the shared apical oxygen atoms in the middle of the bilayer is only present at high pressure. At ambient or low pressure, the symmetry description and hence the scenario presently in this study does not apply to the system.

Acknowledgments. K. J. and F. Z. acknowledge the supports by the National Key R&D Program of China (Grant No. 2022YFA1403900), the National Natural Science Foundation of China (Grant Nos. 11888101, 12174428, and 11920101005), the Strategic Priority Research Program of the Chinese Academy of Sciences (Grant Nos. XDB28000000 and XDB33000000), the New Cornerstone Investigator Program, and the Chinese Academy of Sciences Project for Young Scientists in Basic Research (Grant No. 2022YSBR-048). Z. W. is supported by the U.S. Department of Energy, Basic Energy Sciences (Grant No. DE-FG02-99ER45747).

References

[1] Bednorz J G and Müller K A 1986 *Z. Phys. B-Condens. Matter* **64** 189
[2] Lee P A, Nagaosa N, and Wen X G 2006 *Rev. Mod. Phys.* **78** 17
[3] Keimer B, Kivelson S A, Norman M R, Uchida S, and Zaanen J 2015 *Nature* **518** 179
[4] Maeno Y, Hashimoto H, Yoshida K, Nishizaki S, Fujita T, Bednorz J G, and Lichtenberg F 1994 *Nature* **372** 532
[5] Kamihara Y, Watanabe T, Hirano M, and Hosono H 2008 *J. Am. Chem. Soc.* **130** 3296
[6] Takahashi H, Igawa K, Arii K, Kamihara Y, Hirano M, and Hosono H 2008 *Nature* **453** 376
[7] Paglione J and Greene R L 2010 *Nat. Phys.* **6** 645
[8] Hu J P, Le C, and Wu X 2015 *Phys. Rev. X* **5** 041012
[9] Anisimov V I, Bukhvalov D, and Rice T M 1999 *Phys. Rev. B* **59** 7901
[10] Lee K W and Pickett W E 2004 *Phys. Rev. B* **70** 165109
[11] Chaloupka J and Khaliullin G 2008 *Phys. Rev. Lett.* **100** 016404
[12] Crespin M, Levitz P, and Gatineau L 1983 *J. Chem. Soc. Faraday Trans. 2* **79** 1181
[13] Greenblatt M 1997 *Curr. Opin. Solid State Mater. Sci.* **2** 174
[14] Hayward M A, Green M A, Rosseinsky M J, and Sloan J 1999 *J. Am. Chem. Soc.* **121** 8843
[15] Crespin M, Isnard O, Dubois F, Choisnet J, and Odier P 2005 *J. Solid State Chem.* **178** 1326
[16] Kawai M, Matsumoto K, Ichikawa N, Mizumaki M, Sakata O, Kawamura N, Kimura S, and Shimakawa Y 2010 *Cryst. Growth Des.* **10** 2044
[17] Li D F, Lee K, Wang B Y, Osada M, Crossley S, Lee H R, Cui Y, Hikita Y, and Hwang H Y 2019 *Nature* **572** 624
[18] Osada M, Wang B Y, Lee K, Li D, and Hwang H Y 2020 *Phys. Rev. Mater.* **4** 121801
[19] Li D F, Wang B Y, Lee K, Harvey S P, Osada M, Goodge B H, Kourkoutis L F, and Hwang H Y 2020 *Phys. Rev. Lett.* **125** 027001
[20] Norman M R 2020 *Physics* **13** 85
[21] Sun H L, Huo M W, Hu X W, Li J, Liu Z, Han Y, Tang L, Mao Z, Yang P, Wang B, Cheng J, Yao D X, Zhang G M, and Wang M 2023 *Nature* **621** 493
[22] Hou J, Yang P T, Liu Z Y, Li J Y, Shan P F, Ma L, Wang G, Wang N N, Guo H Z, Sun J P, Uwatoko Y, Wang M, Zhang G M, Wang B S, and Cheng J G 2023 arXiv:2307.09865 [cond-mat.supr-con]
[23] Zhang Y, Su D, Huang Y, Sun H, Huo M, Shan Z, Ye K, Yang Z, Li R, Smidman M, Wang M, Jiao L, and Yuan H 2023 arXiv:2307.14819 [cond-mat.supr-con]
[24] Liu Z, Huo M, Li J, Li Q, Liu Y, Dai Y, Zhou X, Hao J, Lu Y, Wang M, and Wen H H 2023 arXiv:2307.02950 [cond-mat.supr-con]
[25] Luo Z, Hu X, Wang M, Wú W, and Yao D X 2023 *Phys. Rev. Lett.* **131** 126001
[26] Zhang Y, Lin L F, Moreo A, and Dagotto E 2023 *Phys. Rev. B* **108** L180510
[27] Yang Q G, Wang D, and Wang Q H 2023 *Phys. Rev. B* **108** L140505
[28] Sakakibara H, Kitamine N, Ochi M, and Kuroki K 2023 arXiv:2306.06039 [cond-mat.supr-con]
[29] Gu Y, Le C, Yang Z, Wu X, and Hu J 2023 arXiv:2306.07275 [cond-mat.supr-con]
[30] Shen Y, Qin M, and Zhang G M 2023 *Chin. Phys. Lett.* **40** 127401
[31] Christiansson V, Petocchi F, and Werner P 2023 *Phys. Rev. Lett.* **131** 206501
[32] Shilenko D A and Leonov I V 2023 *Phys. Rev. B* **108** 125105

[33] Wú W, Luo Z, Yao D X, and Wang M 2023 arXiv:2307.05662 [cond-mat.str-el]
[34] Cao Y and Yang Y F 2023 arXiv:2307.06806 [cond-mat.supr-con]
[35] Chen X, Jiang P, Li J, Zhong Z, and Lu Y 2023 arXiv:2307.07154 [cond-mat.supr-con]
[36] Liu Y B, Mei J W, Ye F, Chen W Q, and Yang F 2023 *Phys. Rev. Lett.* **131** 236002
[37] Lu C, Pan Z, Yang F, and Wu C 2023 arXiv:2307.14965 [cond-mat.supr-con]
[38] Zhang Y, Lin L F, Moreo A, Maier T A, and Dagotto E 2023 arXiv:2307.15276 [cond-mat.supr-con]
[39] Oh H and Zhang Y H 2023 *Phys. Rev. B* **108** 174511
[40] Liao Z, Chen L, Duan G, Wang Y, Liu C, Yu R, and Si Q 2023 arXiv:2307.16697 [cond-mat.supr-con]
[41] Qu X Z, Qu D W, Chen J, Wu C, Yang F, Li W, and Su G 2023 arXiv:2307.16873 [cond-mat.str-el]
[42] Yang Y F, Zhang G M, and Zhang F C 2023 *Phys. Rev. B* **108** L201108
[43] Fujimori A and Minami F 1984 *Phys. Rev. B* **30** 957
[44] van Elp J, Eskes H, Kuiper P, and Sawatzky G A 1992 *Phys. Rev. B* **45** 1612
[45] Kuiper P, Kruizinga G, Ghijsen J, Sawatzky G A, and Verweij H 1989 *Phys. Rev. Lett.* **62** 221
[46] Taguchi M, Matsunami M, Ishida Y, Eguchi R, Chainani A, Takata Y, Yabashi M, Tamasaku K, Nishino Y, Ishikawa T, Senba Y, Ohashi H, and Shin S 2008 *Phys. Rev. Lett.* **100** 206401
[47] Zhang F C and Rice T M 1988 *Phys. Rev. B* **37** 3759
[48] Coleman P 1984 *Phys. Rev. B* **29** 3035
[49] Anderson P W, Lee P A, Randeria M, Rice T M, Trivedi N, and Zhang F C 2004 *J. Phys.: Condens. Matter* **16** R755
[50] Jiang K, Wu X, Hu J, and Wang Z 2018 *Phys. Rev. Lett.* **121** 227002
[51] Jiang K, Le C, Li Y, Qin S, Wang Z, Zhang F, and Hu J 2021 *Phys. Rev. B* **103** 045108
[52] Yang J, Sun H, Hu X, Xie Y, Miao T, Luo H, Chen H, Liang B, Zhu W, Qu G, Chen C Q, Huo M, Huang Y, Zhang S, Zhang F, Yang F, Wang Z, Peng Q, Mao H, Liu G, Xu Z, Qian T, Yao D X, Wang M, Zhao L, and Zhou X J 2023 arXiv:2309.01148 [cond-mat.supr-con]